

Published in final edited form as:

*Oncogene*. 2016 July 28; 35(30): 4009–4019. doi:10.1038/onc.2015.427.

## **RAD18, WRNIP1 and ATMIN promote ATM signalling in response to replication stress**

**Nnennaya Kanu<sup>1,6</sup>, Tianyi Zhang<sup>1,7</sup>, Rebecca A. Burrell<sup>2</sup>, Atanu Chakraborty<sup>1</sup>, Janet Cronshaw<sup>1</sup>, Clive Da Costa<sup>1</sup>, Eva Grönroos<sup>2</sup>, Helen N. Pemberton<sup>3</sup>, Emma Anderton<sup>3</sup>, Laure Gonzalez<sup>4,8</sup>, Simone Sabbioneda<sup>5</sup>, Helle D. Ulrich<sup>4,8</sup>, Charles Swanton<sup>2</sup>, and Axel Behrens<sup>1,9,\*</sup>**

<sup>1</sup>Mammalian Genetics Laboratory, The Francis Crick Institute, 44 Lincoln's Inn Fields, London WC2A 3LY, UK

<sup>2</sup>Translational Cancer Therapeutics Laboratory, The Francis Crick Institute, 44 Lincoln's Inn Fields, London WC2A 3LY, UK and UCL Cancer Institute, 72 Huntley Street, London WC1E 6BT, UK

<sup>3</sup>Molecular Oncology Laboratory, Cancer Research UK, London Research Institute, 44, Lincoln's Inn Fields, London WC2A 3LY, UK

<sup>4</sup>DNA Damage Tolerance Laboratory, Cancer Research UK, London Research Institute, Clare Hall Laboratories, Blanche Lane, South Mimms, Herts EN6 3LD, UK

<sup>5</sup>Istituto di Genetica Molecolare-CNR, Via Abbiategrosso, 207 - 27100 Pavia, Italy

<sup>9</sup>School of Medicine, King's College London, Guy's Campus, London, SE1 1UL, UK

### **Abstract**

The DNA replication machinery invariably encounters obstacles that slow replication fork progression, and threaten to prevent complete replication and faithful segregation of sister chromatids. The resulting replication stress activates ATR, the major kinase involved in resolving impaired DNA replication. In addition, replication stress also activates the related kinase ATM, which is required to prevent mitotic segregation errors. However, the molecular mechanism of ATM activation by replication stress is not defined. Here we show that monoubiquitinated Proliferating Cell Nuclear Antigen (PCNA), a marker of stalled replication forks, interacts with the ATM cofactor ATMIN via WRN interacting protein 1 (WRNIP1). ATMIN, WRNIP1 and RAD18,

---

Users may view, print, copy, and download text and data-mine the content in such documents, for the purposes of academic research, subject always to the full Conditions of use:[http://www.nature.com/authors/editorial\\_policies/license.html#terms](http://www.nature.com/authors/editorial_policies/license.html#terms)

\***Corresponding author:** Axel Behrens, Mammalian Genetics Lab, The Francis Crick Institute, 44 Lincoln's Inn Fields, London WC2A 3LY, UK, Tel: 44 207 269 3361, Fax: 44 207 269 3581, [axel.behrens@crick.ac.uk](mailto:axel.behrens@crick.ac.uk).

<sup>6</sup>Current address: Translational Cancer Therapeutics Laboratory, UCL Cancer Institute, 72 Huntley Street, London WC1E 6BT, UK

<sup>7</sup>Current address: Institute of Medical Biology, 8A Biomedical Grove, #06-06 Immunos, Singapore 138648

<sup>8</sup>Current address: Institute of Molecular Biology, Ackermannweg 4, D – 55122 Mainz, Germany

#### **Author contributions**

N.K. designed and performed most of the experiments and analysed the data. T.Z., R.A.B., A.C., J.C. and C.D.C. performed experiments. E.G., H.N.P., E.A., and C.S. provided technical assistance. S.S., L.G. and H.D.U. provided reagents and technical assistance. N.K. and A.B. wrote the manuscript.

#### **Conflict of Interest statement**

The authors declare that they have no conflicts of interest.

the E3 ligase responsible for PCNA monoubiquitination, are specifically required for ATM signalling and 53BP1 focus formation induced by replication stress, not ionising radiation. Thus, WRNIP1 connects PCNA monoubiquitination with ATMIN/ATM to activate ATM signalling in response to replication stress and contribute to the maintenance of genomic stability.

## Keywords

ATMIN; ATM; WRNIP1; RAD18

## Introduction

The ataxia telangiectasia mutated (ATM) kinase responds to the presence of DNA damage by activating cell cycle checkpoints and promoting DNA repair<sup>15, 29</sup>. Different stimuli activate ATM via the action of distinct cofactors. Following the induction of double-strand breaks by ionising radiation (IR), the MRN complex (Mre11, Rad50, NBS1) recruits active ATM to the sites of DNA damage<sup>28, 44</sup>. Treatment of cultured cells with hypotonic stress or chloroquine induces ATM autophosphorylation and increased phosphorylation of ATM substrates without detectable DNA damage<sup>2</sup>. Although the MRN subunit NBS1 is required for IR-induced ATM signalling, it is dispensable for signalling in response to hypotonic stress<sup>16</sup>, suggesting that another mechanism of ATM activation operates in this context.

We have since described a second ATM cofactor, ATMIN (ATM Interactor)<sup>25</sup> – also known as ATM/ATR-Substrate Chk2-Interacting zinc finger protein<sup>33</sup> – that has a complementary function to NBS1 with respect to ATM activation: it is dispensable for IR-induced ATM signalling, but required for ATM activation following hypotonic stress. Hence, ATMIN is required for ATM activation in a signal-dependent manner<sup>26</sup>. While the biological function of ATM activation by double-strand breaks and MRN is well established, the role of ATMIN-dependent ATM activation is enigmatic.

Aphidicolin, an inhibitor of replicative DNA polymerases  $\alpha$  and  $\delta$ , causes replication stress by inhibiting the progression of the replisome. Inhibitors of DNA replication stimulate ATM autophosphorylation<sup>2, 16</sup>, indicating that ATM is activated in response to replication stress. Recent work has shown that ATMIN is required for ATM signalling in this context<sup>39</sup>. However, the molecular mechanism responsible for activating ATMIN-dependent ATM signalling in replication stress conditions is unknown.

Stress induced in cycling cells by accumulation of replication-blocking DNA lesions, or any barrier to complete replication, primarily activates the Ataxia Telangiectasia and Rad3-related kinase (ATR) to stabilise the replication fork and promote replication restart<sup>47</sup>. In addition to DNA breaks if replication forks collapse, prolonged replisome stalling may result in the progression to G2 phase of cells with incompletely replicated DNA or unresolved replication intermediates. When these cells undergo mitosis, the segregation of under-replicated DNA during anaphase generates ultrafine DNA bridges. Several proteins, including the BLM helicase and the SNF2-family Plk1-interacting checkpoint helicase (PICH) localise to ultrafine bridges, possibly with the aim of disentangling under-replicated DNA<sup>4, 11, 12</sup>. Replication stress also induces the formation of G1 phase nuclear bodies

containing p53-binding protein 1 (53BP1)<sup>22, 32</sup>. The symmetrical nature of these nuclear bodies in the two daughter cells indicates that they likely mark sister loci from the previous S phase that require further protection or resolution. Importantly, formation of 53BP1 nuclear bodies depends on ATM but not ATR<sup>22, 32</sup>. Thus, activation of ATM in replication stress conditions is likely required to prevent persistent genome instability beyond the original stimulus and into future cell cycles.

Here we identify the molecular components enabling ATM signalling under conditions of replication stress and provide support for replication stress as a cellular trigger for ATMIN-dependent ATM signalling. In response to replication fork stalling, the RAD18 ubiquitin ligase (E3) ubiquitinates the replicative polymerase processivity factor Proliferating Cell Nuclear Antigen (PCNA) at lysine 164<sup>23, 43</sup>. We identify WRN-interacting protein 1 (WRNIP1) as an ATMIN interacting protein and demonstrate that WRNIP1 interacts with RAD18 and with ubiquitinated PCNA, which could recruit ATMIN/ATM to sites of replication stress. Depletion of RAD18, WRNIP1 and ATMIN severely impair ATM signalling in response to replication stress, and ultrafine bridge formation is increased in ATMIN-deficient cells. Thus our work describes a novel mode of ATM activation and signalling that acts in the context of replication stress to protect genomic integrity.

## Results

### Identification of WRNIP1 as an ATMIN binding protein

The ATM interactor ATMIN is required for ATM signalling in stress conditions that do not induce double-strand breaks, such as chloroquine and hypotonic stress<sup>25</sup>, but the pathways involved in such non-canonical ATM activation are poorly understood. We performed a large-scale immunoprecipitation to look for additional ATMIN interactors (Supplementary Fig. 1a) and identified WRN-interacting protein (WRNIP1) by mass spectrometry. The interaction between ATMIN and WRNIP1 was confirmed by co-immunoprecipitation of endogenous proteins (Fig. 1a). We proceeded to investigate the function of ATMIN-WRNIP1 interaction in mammalian cells.

WRNIP1 was shown to localise to RPA foci, which mark areas of single-stranded DNA exposed at replication forks, in untreated cells and to relocalise in response to replication blocking agents<sup>13</sup>, suggesting that it may play a role in facilitating replication. In response to replication fork stalling, PCNA becomes mono-ubiquitinated by the Rad18 E3 ubiquitin ligase, and serves as a platform to recruit translesion synthesis polymerases<sup>24, 48</sup>. Mgs1, the yeast homolog of WRNIP1, binds mono-ubiquitinated PCNA and is subsequently recruited to stalled replication forks<sup>38</sup>. Since replication stress also activates ATM<sup>2, 16, 35</sup>, and since ATMIN was recently shown to be required for efficient ATM activation by replication stress<sup>39</sup>, we asked whether WRNIP1 is required for ATMIN function in ATM signalling in response to replication stalling.

### ATMIN contributes to aphidicolin-induced pATM foci formation

In order to induce replication stalling in cells, we used the polymerase  $\alpha$  and  $\delta$  inhibitor Aphidicolin (Aph). Aphidicolin was originally used to define common fragile sites, DNA

regions that are prone to breakage in response to replication stress<sup>19</sup>. While aphidicolin-induced replication stress did not significantly alter the efficiency of ATMIN/WRNIP1 interaction (Supplementary Fig. 1b), aphidicolin treatment induced the formation of abundant nuclear WRNIP1 foci (Fig. 1b and Supplementary Fig. 1c). The phospho-ATM antibody (pATM) recognises active ATM phosphorylated at serine 1981, and also some similar phospho-epitopes of substrates phosphorylated by ATM, making it a marker of ATM signalling when used for immunofluorescence<sup>30</sup>. Similarly to WRNIP1, pATM staining showed abundant nuclear foci upon aphidicolin treatment. 53BP1, an ATM substrate, formed similar aphidicolin-induced foci (Fig. 1b and Supplementary Fig. 1c). Importantly, pATM and 53BP1 colocalised with WRNIP1 (Fig. 1b, c).

To confirm whether the formation of these aphidicolin-induced foci requires ATMIN, we stained for pATM and 53BP1 in the presence or absence of aphidicolin in *ATMIN*<sup>+/+</sup> and *ATMIN*<sup>-/-</sup> mouse embryonic fibroblasts (MEFs). As previously published in human cells<sup>39</sup>, *ATMIN*<sup>+/+</sup> MEFs formed pATM and 53BP1 foci in response to aphidicolin that largely colocalised (Fig. 1d). However, formation of these foci was significantly reduced in *ATMIN*<sup>-/-</sup> MEFs, suggesting that ATMIN contributes to ATM's response to aphidicolin (Fig. 1d,e). Hydroxyurea-induced formation of pATM foci was also reduced in ATMIN-depleted cells (Supplementary Fig. 1d). This is in agreement with our previous data showing a reduction in hydroxyurea-induced ATM activation in ATMIN-null cells<sup>25</sup>, and supports the hypothesis that ATMIN promotes ATM signalling in response to replication stress.

To examine whether WRNIP1, pATM and 53BP1 colocalise in response to replication stress at the affected genomic sites, we used HeLa cells carrying a stably integrated LacO array and expressing a fluorescently tagged Lac repressor (CherryLacR)<sup>41</sup>. This protein-bound repetitive DNA has been shown to impede replication<sup>37</sup>, thus forming an artificial replication stress site that can be visualised as a single large focus by fluorescence microscopy. In the presence of 0.2  $\mu$ M aphidicolin, WRNIP1, pATM and 53BP1 were all found to colocalise with this site (Fig. 1f,g). Notably, the ubiquitin ligase RAD18, which monoubiquitinates PCNA at stalled replication forks, also colocalised with pATM at the CherryLacR site (Fig. 1f,g), supporting the idea that ATM activity is localised to sites of replication stress.

### WRNIP1 foci formation requires PCNA ubiquitination by RAD18

WRNIP1 is known to bind ubiquitin via its ubiquitin binding Zinc finger (UBZ) domain<sup>5</sup>, and the WRNIP1 yeast homolog Mgs1 is targeted to sites of replication stress via interaction of its UBZ with monoubiquitinated PCNA<sup>38</sup>. In agreement with the yeast findings, we found that WRNIP1 binds to ubiquitinated PCNA (Fig. 2a). Since WRNIP1 does not bind free monoubiquitin<sup>5</sup> and shows only a weak interaction with unmodified PCNA (Fig. 2a), this supports the notion that WRNIP1 preferentially interacts with the monoubiquitinated PCNA protein.

We next investigated if interaction of monoubiquitinated PCNA with the WRNIP1 UBZ domain contributes to WRNIP1 relocalisation into aphidicolin-induced foci. PCNA is monoubiquitinated in response to replication stalling by RAD18, and in response to aphidicolin treatment, WRNIP1 and RAD18 foci colocalised by immunofluorescence

(Supplementary Fig. 2a). Whereas WRNIP1 knock-down had no effect on RAD18 focus formation, the formation of aphidicolin-induced WRNIP1 foci depended on the presence of RAD18 (Supplementary Fig. 2a-c). To test the role of the WRNIP1 ubiquitin binding, we took advantage of a previously described mutation of the UBZ domain, of a highly conserved aspartate residue at position 37 of WRNIP1 (D37A) that abolishes ubiquitin binding<sup>5</sup>. Reconstitution of WRNIP-depleted cells with wild-type siRNA-resistant WRNIP1 restored aphidicolin-induced pATM and 53BP1 foci formation, but the ubiquitin-binding WRNIP1 mutant D37A did not (Fig. 2b,c), suggesting that WRNIP1 interaction with ubiquitin is required for ATM signalling in aphidicolin conditions. Under these conditions of low dose aphidicolin treatment, 83% of S phase cells exhibited prominent WRNIP1 foci when cells were pulsed with EdU for 30 minutes, consistent with WRNIP1 being recruited to sites of replication stress (Fig. 2d and Supplementary Fig. 3a,b). To ask whether ubiquitinated PCNA in particular is required to recruit WRNIP1, we made use of a previously described MRC5 cell line expressing His<sub>6</sub>-PCNA mutated at its ubiquitination site, lysine 164<sup>34</sup>. Following depletion of endogenous PCNA by siRNA (Fig. 2e), PCNA K164R-expressing cells showed reduced WRNIP1 foci compared with similar cells expressing WT PCNA (Fig. 2f,g). Mutant PCNA also showed a reduction in aphidicolin-induced pATM foci and phosphorylation of ATM substrates (Fig. 2h-j). Taken together, these data suggest that Rad18-induced PCNA ubiquitination at K164 and WRNIP1 interaction with the ubiquitinated PCNA are required for proper ATM signalling in response to replication stress.

The defect in P-ATM and 53BP1 foci formation following treatment of ATMIN depleted cells with 0.2 $\mu$ m aphidicolin became noticeable at around 4 hours post treatment. This coincides with the time point when PCNA ubiquitylation was seen to occur (Supplementary Fig. 4a,b). The delay in the kinetics of PCNA ubiquitylation was consistent with a slower progression through S phase (Supplementary Fig. 4a,c).

### **WRNIP1 is not required for IR-induced ATM signalling**

The above data indicate that ATMIN and WRNIP1 contribute to pATM and 53BP1 foci formation in response to aphidicolin. Since these repair foci also form in response to ATM activation at double-strand breaks, we examined pATM and 53BP1 foci formation in response to ionising radiation (IR). As expected, pATM and 53BP1 formed foci in response to IR, however, these foci were unaffected by depletion of ATMIN, WRNIP1 or RAD18 (Fig. 3a-d and Supplementary Fig. 5a). In agreement with the normal IR-induced focus formation, depletion of ATMIN, WRNIP1 or RAD18 had no effect on ATM auto-phosphorylation, or phosphorylation of the ATM substrates Kap1, p53 or Chk2 induced by IR (Fig. 3e). Thus ATMIN, WRNIP1 and RAD18 are dispensable for ATM signalling induced by DSBs.

We next examined ATM signalling in response to aphidicolin in cells depleted of ATMIN, WRNIP1 and RAD18. Depletion of ATMIN by siRNA reduced both pATM and 53BP1 foci in aphidicolin-treated cells (Fig. 4a-c). Depletion of WRNIP1 or RAD18 using siRNA reduced the formation of pATM and 53BP1 foci in aphidicolin conditions to a similar extent as ATMIN depletion, supporting the idea that all three proteins are required to localise ATM

signalling in response to replication stress (Fig. 4a-c). Depletion of ATMIN, WRNIP1 or RAD18 also reduced aphidicolin-stimulated phosphorylation of Kap-1 and P53 (Fig. 4d). The aphidicolin-induced phosphorylation of Kap1 was confirmed to be ATM-dependent (Supplementary Fig. 5b).

Despite the impaired phosphorylation of ATM substrates, phosphorylation of ATM itself in aphidicolin conditions was less affected by depletion of ATMIN, WRNIP1 or RAD18 (Fig. 4e). This result could indicate that ATM is still activated in the absence of ATMIN, WRNIP1 or RAD18 proteins; however, the impaired DDR foci formation in response to replication stress in the absence of RAD18, WRNIP1 and ATMIN supports the notion that ATM is not localised properly in response to aphidicolin treatment, and that this mislocalisation may contribute to impaired ATM substrate phosphorylation.

The requirement for ATMIN, WRNIP1 and RAD18 for foci formation in aphidicolin-treated cells is in contrast to the normal ATM response to IR, suggesting that ATM localisation is differently regulated in the two conditions.

As previously reported<sup>32</sup>, 53BP1 also forms prominent G1 nuclear bodies, which are ATM dependent, in cells following replication stress. To determine whether these bodies also require ATMIN, WRNIP1 and RAD18 for their formation, we quantified the numbers of cells with G1 nuclear bodies (defined as 53BP1 foci that occur in cells negative for cyclin A) in cells following siRNA knockdown of ATMIN, WRNIP1 or RAD18. Despite overall aphidicolin-induced 53BP1 foci being reduced in knockdown cells (Fig. 4c), the proportion of cells with G1 nuclear bodies was not significantly affected by depletion of ATMIN, WRNIP1 or RAD18 (Supplementary Fig. 5c). Thus, ATM is likely activated downstream of replication stress via different mechanisms depending on whether or not cells have progressed to the next cycle.

### **Aphidicolin-induced ATM signalling is mostly independent of ATR**

Aphidicolin treatment inhibits progression of the replicative polymerase but not of the helicase, and therefore increases the amount of single stranded DNA (ssDNA) exposed by helicase unwinding at the replication fork<sup>9</sup>. This ssDNA is coated by RPA, forming foci that mark the sites of replication fork stalling. To see whether WRNIP1 and RAD18 foci form at these sites, we co-stained for WRNIP1 or RAD18 and RPA. Colocalisation of both proteins with RPA was observed in response to aphidicolin treatment, suggesting that WRNIP1 and RAD18 assemble on or near ssDNA (Fig. 5a and Supplementary Fig. 6a). 53BP1 also showed colocalisation with RPA in response to aphidicolin treatment (Fig. 5a and Supplementary Fig. 6a). Since RAD18 is already known to act at stalled forks, this colocalisation also places WRNIP1, 53BP1 and potentially ATMIN and pATM at sites of replication stress.

Since ATR is also activated in response to replication stress, we next asked whether WRNIP1 foci formation or ATM activation is dependent on ATR. Knockdown of ATR by siRNA did not impair WRNIP1 or RAD18 foci formation in aphidicolin-treated cells, suggesting that WRNIP1 and RAD18 recruitment still occurs when ATR levels are reduced (Fig. 5b,c and Supplementary Fig. 6b,c). This result is in agreement with the finding of

Lehmann and colleagues that PCNA ubiquitination is independent of ATR<sup>34</sup>. Importantly, aphidicolin-induced phosphorylation of ATM substrates was not impaired in cells treated with ATR inhibitor (Fig. 5d), nor was formation of pATM or 53BP1 foci impaired by ATR siRNA, though incomplete knockdown of ATR could conceivably mask an effect here (Fig. 5e,f and Supplementary Fig. 6c). This implies that while ATR and ATM are concomitantly activated in response to replication stress, ATM activation does not require full ATR function.

### Impaired ATM signalling increases ultrafine bridges

Faithful segregation of the genetic material during cell division is crucial for maintenance of genome integrity. The two separating sister chromatids must be disentangled before mitosis. However, as a consequence of replication stress, the separating sister chromatids are often connected by DNA bridges in anaphase<sup>8</sup>. After partial inhibition of DNA replication, sister chromatids can become interlinked, primarily at genetic loci with intrinsic replication difficulties, such as fragile sites<sup>11</sup>. Fragile sites are prone to chromosome breakage, deletion, and translocation, and are often associated with cancer and other genetic disorders. Ultrafine bridges (UFBs), a class of anaphase bridges, are refractory to DAPI staining and are bound by several proteins including PICH (Supplementary Fig. 6d)<sup>4, 10</sup>.

Inhibition of ATM or depletion of ATR protein both resulted in a large increase in UFBs (Fig. 5g). A combination of ATM inhibition and ATR depletion had no additive effect. Moreover, depletion of ATMIN also augmented UFB frequency to a similar extent as ATM inhibition (Fig. 5g and Supplementary Fig. 6e). In contrast, depletion of NBS1, which is required for canonical ATM signalling, had little effect (Fig. 5g).

As another readout of unresolved damage remaining after S phase has concluded, we also examined  $\gamma$ H2AX foci in metaphase cells, identified by the condensation of DAPI-stained chromosomes at the metaphase plate. Induction of replication stress using aphidicolin induces  $\gamma$ H2AX foci that persist in metaphase (Fig. 5h and Supplementary Fig. 6f). Depletion of ATMIN or ATM strongly increased metaphase  $\gamma$ H2AX foci (Fig. 5h and Supplementary Fig. 6f). Thus, ATMIN-dependent ATM signalling acts to limit the persistence of unresolved chromosome damage remaining at mitosis.

### Discussion

The canonical mode of ATM activation occurs in response to DNA double-strand breaks. In a landmark paper, Bakkenist and Kastan<sup>2</sup> showed that ATM can also be activated in the absence of detectable breaks by treatment of cells with hypotonic stress or chloroquine. ATMIN is required for this non-canonical mode of ATM signalling<sup>25</sup>, but until now a physiologically relevant stimulus has been elusive. Schmidt et al. recently demonstrated that replication stress is a physiological activator of ATMIN-dependent ATM signalling<sup>39</sup>. In this study we identify the mechanism of ATM activation and recruitment to stalled replication forks. We show that replication stress activates ATMIN-dependent ATM signalling via a mechanism that requires RAD18 and WRNIP1. Although ATM has been shown to be involved in restarting stalled replication forks and in recruiting 53BP1 to fragile

sites <sup>1, 14, 22, 32, 42</sup>, the mechanism by which ATM signalling is activated in the context of replication stress has been enigmatic.

Ubiquitination of PCNA, which travels with the replication fork, is a key molecular event triggered by replication fork stalling. Ubiquitinated PCNA recruits numerous proteins to stalled forks, principally by interaction of the attached ubiquitin moieties with the ubiquitin interaction domains of PCNA-interacting proteins <sup>43</sup>. In yeast, ubiquitinated PCNA was shown to recruit Mgs1, the yeast homolog of WRNIP1, specifically to sites of stalled replication <sup>38</sup>. This mode of recruitment appears to be evolutionarily conserved, as we found that mammalian WRNIP1 is also recruited to sites of replication stress (aphidicolin-induced foci marked by RPA and RAD18) in a RAD18-dependent manner. WRNIP1 recruitment to these sites is dependent on its UBZ domain, which was previously shown to bind mono- and poly-ubiquitin <sup>6, 13</sup>. Our study suggests an important biological function of mammalian WRNIP1 in recruiting and activating ATM through interaction with ATMIN. No currently available antibodies reliably detect endogenous ATMIN in immunofluorescence experiments. However, GFP-tagged ATMIN colocalizes with WRNIP1, and overexpression of GFP-ATMIN increases WRNIP1 foci formation (data not shown). Because ATMIN is required for pATM and 53BP1 foci formation at replication stress sites, and interacts with both WRNIP1 and ATM, we speculate that ATMIN may also relocalise to sites of replication damage. Our data suggest that WRNIP1 acts as a bridging factor connecting ubiquitinated PCNA and ATMIN/ATM. However, it is likely that additional protein-protein interactions may stabilise ATM recruitment at sites of replication stress, such as the described interaction of WRNIP1 with the WRN protein, and of ATM with PCNA <sup>18, 27, 46</sup>.

We have previously shown that ATMIN is dispensable for ATM signalling in response to ionising radiation <sup>25, 31</sup>. Importantly, the formation of 53BP1 foci in response to IR, and the IR-induced phosphorylation of ATM substrates, is also normal in cells lacking WRNIP1 and RAD18 (Fig. 3). Thus ATM activation by double-strand breaks and by replication stress is mediated by two distinct molecular pathways, which are characterised by the MRN complex and WRNIP1, ATMIN and RAD18 (WAR) proteins, respectively (Supplementary Figure 7). Each arm of the ATM signalling pathway serves to protect genomic integrity. MRN-dependent ATM signalling functions to repair double-strand breaks whereas WAR-dependent ATM signalling acts in response to replication stress.

At present the precise function of ATM signalling in replication stress conditions is unclear. It has been suggested that ATM promotes repair and restart of collapsed forks that have already been converted to double-strand breaks, aligning its role in replication with the canonical break-induced signalling pathway <sup>7, 40</sup>. Although our data do not exclude this role, the requirement for the WAR proteins, which are not required for ATM activation at double-strand breaks, suggests that a different DNA structure contributes to ATM activation in this context. Indeed, a recent study has shown that the helicase FBH1, involved in replication fork reversal, is required for ATM activation in conditions of replication fork stalling <sup>17</sup>.

Aphidicolin treatment causes an increase in UFBs and anaphase bridges, presumably because the replication stress lesions induced exceed the immediate cellular repair capability. Although UFBs can still be safely resolved at anaphase, there is a higher risk of

chromosome missegregation if this fails and so other repair and/or decatenation mechanisms are preferentially used to separate sister chromatids before this stage, up to and including cleavage of unreplicated loci<sup>45</sup>. Depletion of ATMIN or inhibition of ATM also leads to a notable increase in UFBs (Fig. 5g), suggesting that the ATM signalling pathway is required to deal with DNA damage normally occurring during S phase and thus limits UFB formation. Our observation that ATMIN deficiency predisposes cells to a high incidence of UFBs and DNA damage that persists in metaphase could be linked to the genome instability and subsequent accelerated tumour development seen in B cell specific ATMIN knock-out mice<sup>31</sup>. Further work will be needed to establish whether ATM signalling mediated by the WAR proteins contributes to ATM's function in cancer suppression. Oncogene-induced replication stress and associated activation of the DNA damage response including ATM is thought to be a barrier to tumour formation<sup>3, 20, 21</sup>, but it is currently not clear whether ATMIN, WRNIP1 and RAD18 also contribute to ATM activation in response to oncogene-induced replication stress. If so, this would underline the importance of alternative mechanisms of ATM activation for genome stability and tumour suppression.

## Materials & Methods

### Cell culture and treatment

*ATMIN*<sup>+/+</sup> and *ATMIN*<sup>-/-</sup> MEFs were derived from E12.5 embryos resulting from heterozygous *ATMIN*<sup>+/-</sup> intercrosses. MRC-5 cells stably expressing either WT or K164R PCNA<sup>34</sup> were provided by S. Sabbioneda. HEK293, HeLa and HCT116 cells were provided by Cancer Research UK Cell Services, which performs authentication and mycoplasma testing. HeLa cells carrying a stably integrated LacO array and expressing CherryLacR were a kind gift from E. Soutoglou<sup>41</sup>. MEFs, MRC-5, HEK293, HeLa and HCT116 cells were cultured in DMEM supplemented with 10% FCS. MRC-5 cell culture medium was supplemented with 0.6mg/ml G418 to maintain expression of the transgene. Cells were cultured at 37°C with 5% CO<sub>2</sub> and either 3% or 20% oxygen. Where indicated cells were treated with 0.2µM aphidicolin (Sigma) for 24 hours or 2µM aphidicolin for 1 hour. IR experiments were performed using a Cs-137 gamma irradiator at 2.1 Gy min<sup>-1</sup>. Plasmid DNA transfections were performed using Lipofectamine 2000 (Life Technologies) and siRNA transfections using Dharmafect 1 reagent (Dharmacon) both according to the manufacturer's instructions. ATMIN (M-020304-01), WRNIP1 (M-010072-2 or D-010072-18 for Fig. 2b,c), RAD18 (M-004591-00), ATR (M-003202-05), ATM (M-003201-04) and RISC-free control (D-001220-01) siRNAs were obtained from Dharmacon. Q-PCR primers used to assess knockdown of ATMIN, WRNIP1 and RAD18 were: ATMIN forward ccgaattctactgctgtcca; ATMIN reverse cattgtgcttctctcagca; WRNIP1 forward tgatgagattcatcggttcaa; WRNIP1 reverse gagtgatgctccacattcc; RAD18 forward cagctgtttatcacgcgaag; RAD18 reverse taaatcacgatcagagacaaa. MRC5V1 cells stably expressing normal levels of siRNA-resistant wild-type PCNA or PCNA-K164R tagged with 6× histidine residues were transfected with 40nM PCNA siRNA GCCGAGAUCUCAGCCAUAUTT or non-targeting control (Dharmacon). After 72 hours cells were either left untreated or exposed to 0.2 µM aphidicolin for 24 hours. Where indicated cells were treated with the ATM inhibitor (KU55933, 10µM for 24 hours) or pre-treated with ATR inhibitor (VE-821, 1 µM for 1 hour).

## Western blotting

Cells were extracted in 20mM Tris, pH7.5, 150mM NaCl, 0.1% NP-40, 10% glycerol (lysis buffer) supplemented with protease inhibitors (Sigma). Protein samples were separated by SDS-PAGE, and subsequently transferred onto polyvinylidene difluoride membranes. All primary antibodies were used at 1:1000 dilution and secondary antibodies at 1:2000 unless otherwise indicated. The following antibodies were used: ATMIN (AB3271, Millipore, used at 1:5000), WRNIP1 (ab4731, AbCam, used at 1:10,000), RAD18 (S2980, Epitomics) pS1981-ATM (10H11.E12, Cell Signalling Technology), ATM (2C1, Santa Cruz), p-T1989-ATR (GTX128145, GeneTex), ATR (sc28901, Santa Cruz), pS824-Kap1 (Bethyl Laboratories), Kap1 (Bethyl Laboratories), p-S317-Chk1 (2344, Cell Signalling Technology), Chk1 (sc8408, Santa Cruz), p-S966-Smc1 (A300-050A, Bethyl Laboratories), Smc1 (ab9262, AbCam), p53 (DO-1, Santa Cruz), pS15-p53 (Cell Signalling Technology), pT68-Chk2 (Cell Signalling Technology), Chk2 (Clone 7, Millipore), pS33-RPA (A300-246A, Bethyl Laboratories), RPA (sc56770, Santa Cruz), Ub-PCNA (Lys 164) (13439, Cell Signaling Technology), PCNA (2586, Cell Signaling Technology), PCNA-HRP (Clone PC10, sc56 Santa Cruz), His (A00186-100, Genscript), Flag M2 (Sigma), c-Myc (Sigma),  $\beta$ -actin (Sigma), alpha-tubulin (ab7291, AbCam), GAPDH-HRP (ab9385, Abcam) and HRP-conjugated goat anti-mouse/rabbit IgG (Sigma).

## Immunoprecipitation

Lysates were precleared for 1 hr by rotation at 4°C, and proteins were immunoprecipitated overnight with the indicated antibodies. Immunocomplexes were subsequently captured by rotation for 2 hrs with protein A- and protein G-Sepharose beads (Sigma). Alternatively proteins were immunoprecipitated from precleared lysates using the relevant antibody-agarose conjugate. Immunoprecipitates were washed three times with lysis buffer, and samples were processed for Western blotting as above.

## Nickel-nitrilotriacetic acid pulldown

Ubiquitinated human PCNA was prepared by in vitro monoubiquitination of purified PCNA using His-tagged ubiquitin and purified by Nickel-nitrilotriacetic acid ( $\text{Ni}^{2+}$ -NTA) affinity chromatography using the methods of Parker and Ulrich<sup>36</sup>. 1 $\mu$ g FLAG-WRNIP was incubated with 1 $\mu$ g His-PCNA or 1 $\mu$ g ubiquitinated (Ub-)His-PCNA for 1 hr at 4°C in binding buffer (20mM Tris-HCl pH7.5, 150mM NaCl, 1mM EDTA, 0.2% NP-40, 30mM imidazole). His-PCNA was pulled down with  $\text{Ni}^{2+}$ -NTA agarose beads and washed thrice with increasing concentrations of imidazole (50 mM, 80 mM and 100 mM). Samples were separated on 4-12% Bis-Tris gels (Invitrogen) and immunoblotted with anti-FLAG (Sigma) and anti-PCNA (CR-UK monoclonal) antibodies.

## Immunofluorescence

Primary MEFs and HEK293A cells were adhered onto slides and treated as indicated and fixed with 4% PFA. For MRC-5 cells stably expressing exogenous WT or mutant PCNA, endogenous PCNA was depleted by siRNA (GCCGAGAUCUCAGCCAUAU) before aphidicolin treatment and fixing. For PICH stains, cells were fixed in PTEMF buffer (20mM Pipes, 2 % Triton X-100, 10mM EGTA, 2mM  $\text{MgCl}_2$ , 4% formaldehyde). Antibodies used

were pS1981-ATM (10H11.E12, Cell Signalling Technology), 53BP1 (H-200, Santa Cruz), RPA (Sigma), WRNIP1 (N-17, Santa Cruz), PICH (Millipore), p-S139-H2AX (05-636, Upstate), RAD18 (H00056852-M01, Novus Biologicals), ATR (sc28901, Santa Cruz), Cyclin A (in-house antibody) and FITC/cy3/cy5-conjugated goat anti-mouse/rabbit IgG (H&L) (Jackson). All antibodies were used at 1:100 dilution except p-S139-H2AX (used at 1:400).

### Flow Cytometry

Cells were incubated with 10  $\mu$ M 5-Ethynyl-2'-deoxyuridine (EdU) for the last 30 minutes of aphidicolin treatment. Cell pellets were subsequently washed and fixed with 4% paraformaldehyde for 15 minutes at room temperature. Cells were stained with the Click-iT EdU Cell Proliferation Assay Kit (Invitrogen) according to the manufacturer's instructions and analysed on a BD LSRFortessa (BD Biosciences).

### Microscope image acquisition

Microscope images were taken using a Zeiss axiovert 200M confocal microscope equipped with LSM 510 3 channel confocal imaging system, and a Zeiss 63 $\times$ /1.4 DIC Plan-Apochromat, oil immersion objective lens at 25°C. Cells were stained using AlexaFluor 488 donkey anti-mouse IgG (A21202), AlexaFluor 546 donkey anti-rabbit (A10040), and AlexaFluor 647 donkey anti-goat IgG (A21447) (Invitrogen). Images were acquired using Zeiss LSM 510 ver3.2 software, and processed using Image J to colour split/merge channels.

### Mass spectrometry

HEK293T cells were resuspended in lysis buffer (20mM Tris, pH7.5, 150mM NaCl, 0.1% NP-40), sonicated and precleared. IP was performed with 1.6 g of protein using either ATMIN (Millipore) or rabbit IgG antibody as control overnight at 4°C. Immunocomplexes were captured with Protein A/G and were washed 8 times with lysis buffer prior to elution with 2 $\times$  lithium dodecyl sulfate NuPAGE® buffer. Eluate was loaded on 4-12% Bis-Tris polyacrylamide gels and stained with colloidal Coomassie prior to identification of candidate interacting proteins by mass spectrometry. Excised gel bands were de-stained in 50% acetonitrile (ACN) (Rathburn)/50% 10mM triethylammonium bicarbonate (TEAB) (Sigma), reduced with 10mM dithiothreitol (DTT) (Sigma), alkylated with 50mM iodoacetamide, washed in 10mM TEAB and dehydrated before digestion with 50ng porcine trypsin (Promega) for 16 hours at 37°C. Digests were freeze-thawed, sonicated in 10% ACN/5% formic acid (BDH, UK) and the extract concentrated to dryness in a SpeedVac (ThermoSavant). The dried digest was reconstituted in 1% formic acid and analysed via electrospray on a QTOF 6510 mass spectrometer with Chip Cube™ source interface and 1200 series HPLC running MassHunter B.01.03 (Agilent, USA). MS data was acquired in the 290-2500 m/z range at a scan rate of 6 spectra/second and MSMS data in the 57-3000 m/z range at a scan rate of 4 spectra/second. Data was exported as mzdata.xml within the MassHunter qualitative analysis software and searched against the NCBI nr 20080210 database, on a Mascot in-house server version 2.2.04 (Matrix Science, UK) using Mascot Daemon version 2.2.2 (Matrix Science, UK). The Mascot generated search result files were loaded into Scaffold software 2.1 (Proteome Science, USA).

## Supplementary Material

Refer to Web version on PubMed Central for supplementary material.

## Acknowledgements

Support was given from Mass Spectrometry, Bioinformatics and Biostatistics and the Equipment Park in the Cancer Research UK London Research Institute (now part of the Francis Crick Institute). We are grateful to J. L. Parker in the Ulrich laboratory for preparing ubiquitinated PCNA. R. Bish, I. Dikic, M. Myers, E. Soutoglou and A. Lehmann kindly provided experimental materials. N.K. is funded by the Breast Cancer Research Foundation. T.Z. was financially supported by an A\*STAR NSS-PhD scholarship (Singapore). This work was supported by an ERC grant (281661 ATMINDDDR) to A.B.

## References

1. Ammazalorso F, Pirzio LM, Bignami M, Franchitto A, Pichierri P. ATR and ATM differently regulate WRN to prevent DSBs at stalled replication forks and promote replication fork recovery. *The EMBO journal*. 2010; 29:3156–3169. [PubMed: 20802463]
2. Bakkenist CJ, Kastan MB. DNA damage activates ATM through intermolecular autophosphorylation and dimer dissociation. *Nature*. 2003; 421:499–506. [PubMed: 12556884]
3. Bartkova J, Horejsi Z, Koed K, Kramer A, Tort F, Zieger K, et al. DNA damage response as a candidate anti-cancer barrier in early human tumorigenesis. *Nature*. 2005; 434:864–870. [PubMed: 15829956]
4. Baumann C, Korner R, Hofmann K, Nigg EA. PICH, a centromere-associated SNF2 family ATPase, is regulated by Plk1 and required for the spindle checkpoint. *Cell*. 2007; 128:101–114. [PubMed: 17218258]
5. Bish RA, Myers MP. Werner helicase-interacting protein 1 binds polyubiquitin via its zinc finger domain. *The Journal of biological chemistry*. 2007; 282:23184–23193. [PubMed: 17550899]
6. Bish RA, Fregoso OI, Piccini A, Myers MP. Conjugation of complex polyubiquitin chains to WRNIP1. *Journal of proteome research*. 2008; 7:3481–3489. [PubMed: 18613717]
7. Blackford AN, Schwab RA, Nieminuszczy J, Deans AJ, West SC, Niedzwiedz W. The DNA translocase activity of FANCM protects stalled replication forks. *Human molecular genetics*. 2012; 21:2005–2016. [PubMed: 22279085]
8. Burrell RA, McClelland SE, Endesfelder D, Groth P, Weller MC, Shaikh N, et al. Replication stress links structural and numerical cancer chromosomal instability. *Nature*. 2013; 494:492–496. [PubMed: 23446422]
9. Byun TS, Pacek M, Yee MC, Walter JC, Cimprich KA. Functional uncoupling of MCM helicase and DNA polymerase activities activates the ATR-dependent checkpoint. *Genes & development*. 2005; 19:1040–1052. [PubMed: 15833913]
10. Chan KL, North PS, Hickson ID. BLM is required for faithful chromosome segregation and its localization defines a class of ultrafine anaphase bridges. *The EMBO journal*. 2007; 26:3397–3409. [PubMed: 17599064]
11. Chan KL, Palmal-Pallag T, Ying S, Hickson ID. Replication stress induces sister-chromatid bridging at fragile site loci in mitosis. *Nature cell biology*. 2009; 11:753–760. [PubMed: 19465922]
12. Chan KL, Hickson ID. New insights into the formation and resolution of ultrafine anaphase bridges. *Semin Cell Dev Biol*. 2011; 22:906–912. [PubMed: 21782962]
13. Crosetto N, Bienko M, Hibbert RG, Perica T, Ambrogio C, Kensche T, et al. Human Wrnip1 is localized in replication factories in a ubiquitin-binding zinc finger-dependent manner. *The Journal of biological chemistry*. 2008; 283:35173–35185. [PubMed: 18842586]
14. Davalos AR, Kaminker P, Hansen RK, Campisi J. ATR and ATM-dependent movement of BLM helicase during replication stress ensures optimal ATM activation and 53BP1 focus formation. *Cell cycle*. 2004; 3:1579–1586. [PubMed: 15539948]

15. Derheimer FA, Kastan MB. Multiple roles of ATM in monitoring and maintaining DNA integrity. *FEBS Lett.* 2010; 584:3675–3681. [PubMed: 20580718]
16. Difilippantonio S, Celeste A, Fernandez-Capetillo O, Chen HT, Reina San Martin B, Van Laethem F, et al. Role of Nbs1 in the activation of the Atm kinase revealed in humanized mouse models. *Nature cell biology.* 2005; 7:675–685. [PubMed: 15965469]
17. Fugger K, Mistrik M, Neelsen KJ, Yao Q, Zellweger R, Kousholt AN, et al. FBH1 Catalyzes Regression of Stalled Replication Forks. *Cell reports.* 2015
18. Gamper AM, Choi S, Matsumoto Y, Banerjee D, Tomkinson AE, Bakkenist CJ. ATM protein physically and functionally interacts with proliferating cell nuclear antigen to regulate DNA synthesis. *The Journal of biological chemistry.* 2012; 287:12445–12454. [PubMed: 22362778]
19. Glover TW, Berger C, Coyle J, Echo B. DNA polymerase alpha inhibition by aphidicolin induces gaps and breaks at common fragile sites in human chromosomes. *Hum Genet.* 1984; 67:136–142. [PubMed: 6430783]
20. Gorgoulis VG, Vassiliou LV, Karakaidos P, Zacharatos P, Kotsinas A, Liloglou T, et al. Activation of the DNA damage checkpoint and genomic instability in human precancerous lesions. *Nature.* 2005; 434:907–913. [PubMed: 15829965]
21. Halazonetis TD, Gorgoulis VG, Bartek J. An oncogene-induced DNA damage model for cancer development. *Science.* 2008; 319:1352–1355. [PubMed: 18323444]
22. Harrigan JA, Belotserkovskaya R, Coates J, Dimitrova DS, Polo SE, Bradshaw CR, et al. Replication stress induces 53BP1-containing OPT domains in G1 cells. *J Cell Biol.* 2011; 193:97–108. [PubMed: 21444690]
23. Hoege C, Pfander B, Moldovan GL, Pyrowolakis G, Jentsch S. RAD6-dependent DNA repair is linked to modification of PCNA by ubiquitin and SUMO. *Nature.* 2002; 419:135–141. [PubMed: 12226657]
24. Kannouche PL, Wing J, Lehmann AR. Interaction of human DNA polymerase eta with monoubiquitinated PCNA: a possible mechanism for the polymerase switch in response to DNA damage. *Molecular cell.* 2004; 14:491–500. [PubMed: 15149598]
25. Kanu N, Behrens A. ATMIN defines an NBS1-independent pathway of ATM signalling. *The EMBO journal.* 2007; 26:2933–2941. [PubMed: 17525732]
26. Kanu N, Behrens A. ATMINstrating ATM signalling: regulation of ATM by ATMIN. *Cell cycle.* 2008; 7:3483–3486. [PubMed: 19001856]
27. Kawabe Y, Branzei D, Hayashi T, Suzuki H, Masuko T, Onoda F, et al. A novel protein interacts with the Werner's syndrome gene product physically and functionally. *The Journal of biological chemistry.* 2001; 276:20364–20369. [PubMed: 11301316]
28. Lee JH, Paull TT. ATM activation by DNA double-strand breaks through the Mre11-Rad50-Nbs1 complex. *Science.* 2005; 308:551–554. [PubMed: 15790808]
29. Lee JH, Paull TT. Activation and regulation of ATM kinase activity in response to DNA double-strand breaks. *Oncogene.* 2007; 26:7741–7748. [PubMed: 18066086]
30. Lilley CE, Chaurushiya MS, Boutell C, Landry S, Suh J, Panier S, et al. A viral E3 ligase targets RNF8 and RNF168 to control histone ubiquitination and DNA damage responses. *The EMBO journal.* 2010; 29:943–955. [PubMed: 20075863]
31. Loizou JI, Sancho R, Kanu N, Bolland DJ, Yang F, Rada C, et al. ATMIN is required for maintenance of genomic stability and suppression of B cell lymphoma. *Cancer cell.* 2011; 19:587–600. [PubMed: 21575860]
32. Lukas C, Savic V, Bekker-Jensen S, Doil C, Neumann B, Pedersen RS, et al. 53BP1 nuclear bodies form around DNA lesions generated by mitotic transmission of chromosomes under replication stress. *Nature cell biology.* 2011; 13:243–253. [PubMed: 21317883]
33. McNeese CJ, Conlan LA, Tennis N, Heierhorst J. ASCIZ regulates lesion-specific Rad51 focus formation and apoptosis after methylating DNA damage. *The EMBO journal.* 2005; 24:2447–2457. [PubMed: 15933716]
34. Niimi A, Brown S, Sabbioneda S, Kannouche PL, Scott A, Yasui A, et al. Regulation of proliferating cell nuclear antigen ubiquitination in mammalian cells. *Proceedings of the National Academy of Sciences of the United States of America.* 2008; 105:16125–16130. [PubMed: 18845679]

35. Olcina MM, Foskolou IP, Anbalagan S, Senra JM, Pires IM, Jiang Y, et al. Replication Stress and Chromatin Context Link ATM Activation to a Role in DNA Replication. *Molecular cell*. 2013; 52:758–766. [PubMed: 24268576]
36. Parker JL, Ulrich HD. In vitro PCNA modification assays. *Methods Mol Biol*. 2012; 920:569–589. [PubMed: 22941628]
37. Payne BT, van Knippenberg IC, Bell H, Filipe SR, Sherratt DJ, McGlynn P. Replication fork blockage by transcription factor-DNA complexes in *Escherichia coli*. *Nucleic acids research*. 2006; 34:5194–5202. [PubMed: 17000639]
38. Saugar I, Parker JL, Zhao S, Ulrich HD. The genome maintenance factor Mgs1 is targeted to sites of replication stress by ubiquitylated PCNA. *Nucleic acids research*. 2012; 40:245–257. [PubMed: 21911365]
39. Schmidt L, Wiedner M, Velimezi G, Prochazkova J, Owusu M, Bauer S, et al. ATMIN is required for the ATM-mediated signaling and recruitment of 53BP1 to DNA damage sites upon replication stress. *DNA repair*. 2014; 24:122–130. [PubMed: 25262557]
40. Sirbu BM, Couch FB, Feigerle JT, Bhaskara S, Hiebert SW, Cortez D. Analysis of protein dynamics at active, stalled, and collapsed replication forks. *Genes & development*. 2011; 25:1320–1327. [PubMed: 21685366]
41. Soutoglou E, Dorn JF, Sengupta K, Jasin M, Nussenzweig A, Ried T, et al. Positional stability of single double-strand breaks in mammalian cells. *Nature cell biology*. 2007; 9:675–682. [PubMed: 17486118]
42. Treznik K, Smith E, Smith S, Costanzo V. ATM and ATR promote Mre11 dependent restart of collapsed replication forks and prevent accumulation of DNA breaks. *The EMBO journal*. 2006; 25:1764–1774. [PubMed: 16601701]
43. Ulrich HD. Regulating post-translational modifications of the eukaryotic replication clamp PCNA. *DNA repair*. 2009; 8:461–469. [PubMed: 19217833]
44. Uziel T, Lerenthal Y, Moyal L, Andegeko Y, Mittelman L, Shiloh Y. Requirement of the MRN complex for ATM activation by DNA damage. *The EMBO journal*. 2003; 22:5612–5621. [PubMed: 14532133]
45. Ying S, Minocherhomji S, Chan KL, Palmal-Pallag T, Chu WK, Wass T, et al. MUS81 promotes common fragile site expression. *Nature cell biology*. 2013; 15:1001–1007. [PubMed: 23811685]
46. Yoshimura A, Seki M, Kanamori M, Tateishi S, Tsurimoto T, Tada S, et al. Physical and functional interaction between WRNIP1 and RAD18. *Genes Genet Syst*. 2009; 84:171–178. [PubMed: 19556710]
47. Zeman MK, Cimprich KA. Causes and consequences of replication stress. *Nature cell biology*. 2013; 16:2–9. [PubMed: 24366029]
48. Zhang Z, Zhang S, Lin SH, Wang X, Wu L, Lee EY, et al. Structure of monoubiquitinated PCNA: implications for DNA polymerase switching and Okazaki fragment maturation. *Cell cycle*. 2012; 11:2128–2136. [PubMed: 22592530]

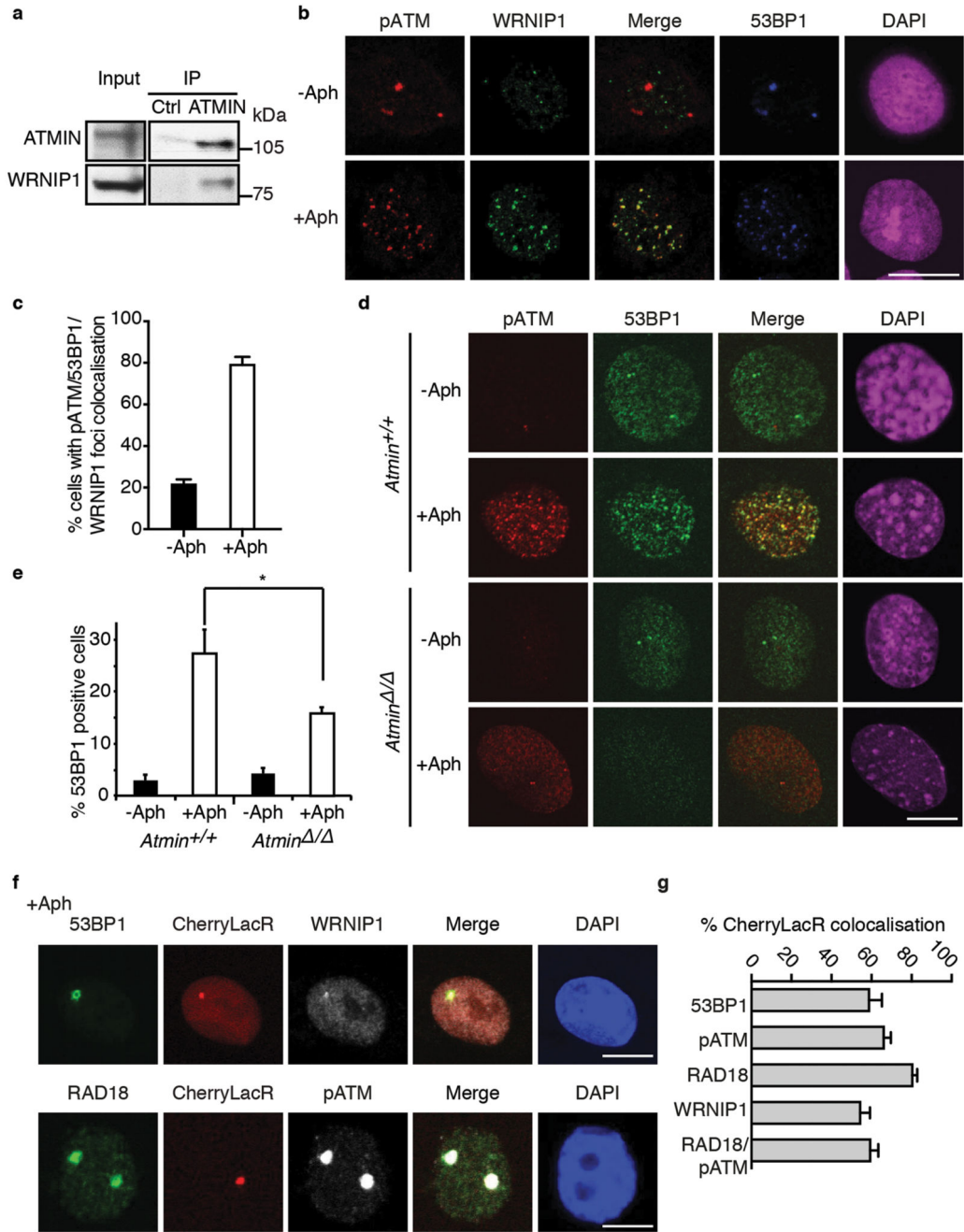


**Figure 1. ATMIN interacts with WRNIP1 and is required for ATM signalling in replication stress conditions**

(a) Co-IP of endogenous ATMIN and WRNIP1. (b) Colocalisation of WRNIP1 and pATM-S1981 (pATM) foci in HEK293 cells in response to 0.2  $\mu$ M aphidicolin for 24 hours.

Experiment was replicated 3 times. (c) Quantification of cells in (b) with pATM/WRNIP1/53BP1 colocalisation. (d) pATM and 53BP1 immunofluorescent staining of control (+/+) and ATMIN-deficient ( / ) MEFs, either untreated (-Aph) or treated with 2  $\mu$ M aphidicolin for 2 hrs (+Aph). (e) Percentage of cells displaying aphidicolin-induced 53BP1 foci (\*P<0.05, t-test). Counts represent 200 cells from three independent

experiments. (f) Colocalisation of 53BP1 and WRNIP1 with a LacO array, marked by CherryLacR. Cells were treated with 0.2  $\mu$ M aphidicolin for 18 hours. (g) Percentage of foci colocalising with CherryLacR from the experiment in (f). Scale bars represent 10 $\mu$ m. Error bars represent s.d.

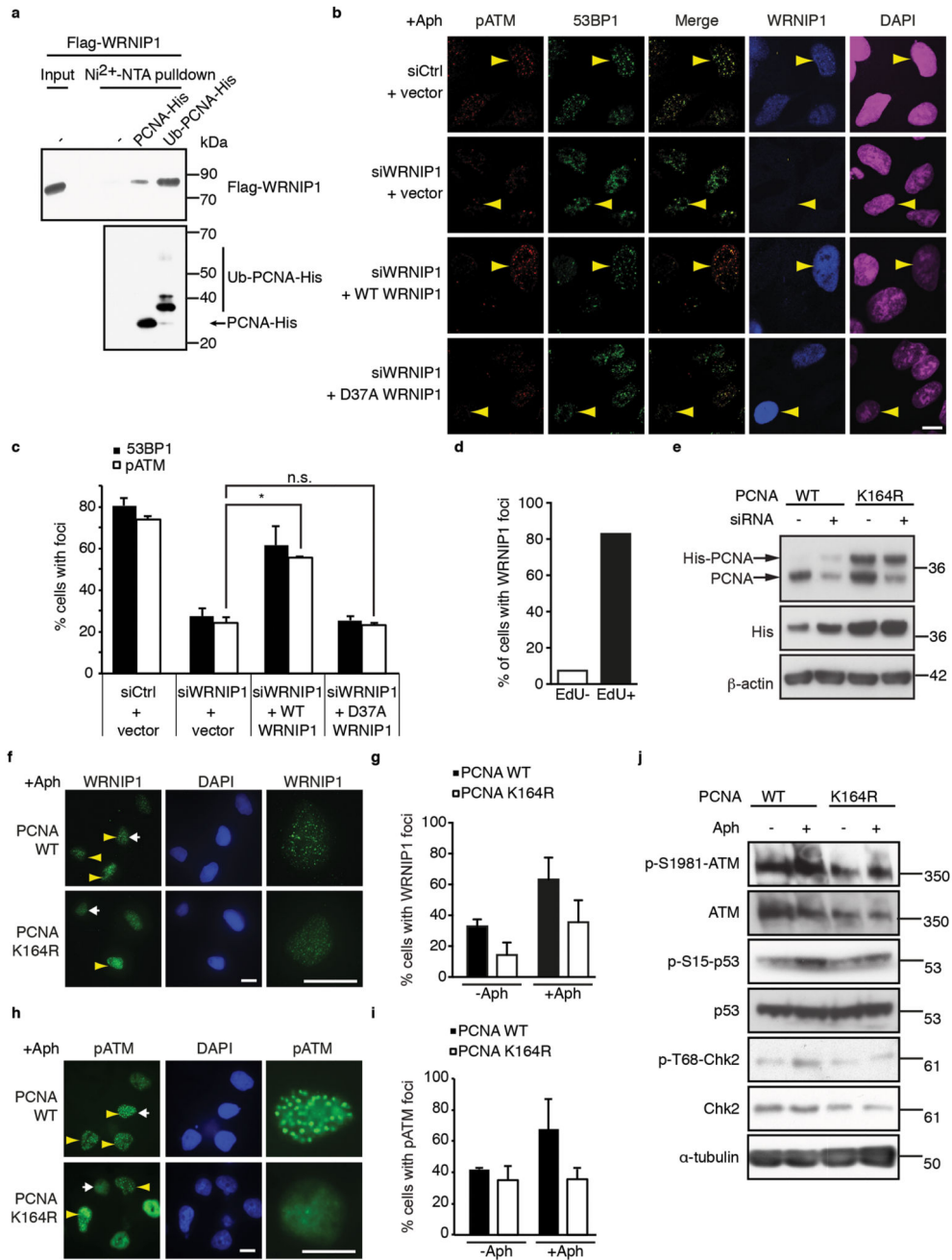


**Figure 2. WRNIP1 binds ubiquitinated PCNA and PCNA ubiquitination is required for aphidicolin-induced foci formation**

(a) Flag-WRNIP1 preferentially interacts with ubiquitinated over unmodified PCNA, shown by Western blotting of Ni<sup>2+</sup>-NTA pulldowns of His-PCNA from mixtures of equal amounts of purified proteins incubated together for 1hr. (b, c) pATM and 53BP1 foci re-establishment in HEK293 cells after treatment with an siRNA pool targeting the 3'UTR of WRNIP1 (siWRNIP1) and subsequent transfection with either empty vector or an expression construct for Flag-tagged WT WRNIP1 or the D37A UBZ mutant. Cells were treated with 0.2  $\mu$ M aphidicolin for 24 hours. Experiment was repeated twice. \*p=0.05 (t-test). n.s., not

significant. Yellow arrowheads in (b) identify example nuclei across rows. In the rescue experiments (lower two rows), WRNIP1 staining indicates transfected cells. (d) Percentage of EdU-positive and EdU-negative HEK293 cells with prominent WRNIP1 foci after 0.2 $\mu$ M aphidicolin for 24 hours. EdU pulse was for the last 30 minutes in aphidicolin before fixing. (e) Western blots showing PCNA levels in MRC-5 cells stably expressing His-tagged siRNA-resistant WT PCNA or PCNA K164R, before and after siRNA depletion of endogenous PCNA. (f) MRC-5 cells stably expressing WT PCNA or PCNA K164R, siRNA-depleted of endogenous PCNA, and treated with 0.2 $\mu$ M aphidicolin for 24 hours, stained with WRNIP1. Yellow arrowheads indicate cells scored as positive for WRNIP1 foci. White arrow indicates cell magnified at right. High magnification images indicate examples of nuclei scored as positive (upper) and negative (lower). (g) Quantification of cells displaying WRNIP1 foci in the experiment in (f). (h) MRC-5 cells stably expressing WT PCNA or PCNA K164R, siRNA-depleted of endogenous PCNA, and treated with 0.2 $\mu$ M aphidicolin for 24 hours, stained with pATM. Yellow arrowheads indicate cells scored as positive for pATM foci. White arrow indicates cell magnified at right. High magnification images indicate examples of nuclei scored as positive (upper) and negative (lower). (i) Quantification of cells displaying pATM foci in the experiment in (h). 100-200 cells were counted per condition. (j) Impaired ATM substrate phosphorylation in response to 2 $\mu$ M aphidicolin treatment for 2 hours in PCNA K164R-expressing cells. Scale bars represent 10 $\mu$ m. Error bars represent s.d.

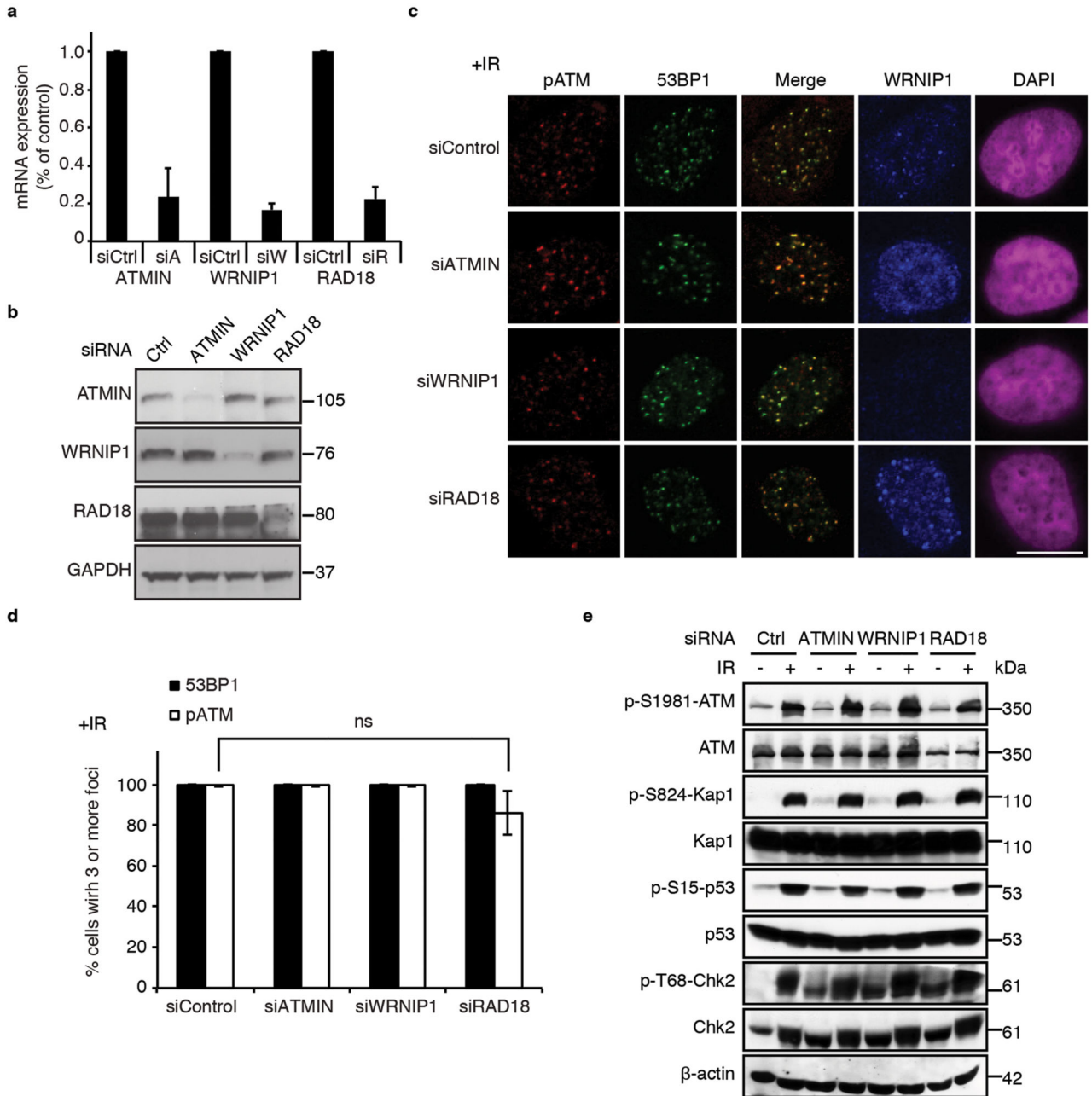


**Figure 3. WRNIP1, ATMIN, and RAD18 are dispensable for ATM signalling in response to ionising radiation**

(a) Relative levels of ATMIN, WRNIP1 and RAD18 mRNA in HEK293 cells treated with non-targeting siRNA (siCtrl) or siRNA against ATMIN (siA), WRNIP1 (siW) or RAD18 (siR) measured by quantitative PCR. Error bars indicate s.d. (b) Western blots showing knockdown of ATMIN, WRNIP1 and RAD18 using the siRNAs in (a). (c) HEK293 cells treated with the indicated siRNAs, exposed to 2 Gy ionising radiation (IR), fixed after 30 mins and stained with antibodies against 53BP1, pATM and WRNIP1. Scale bar indicates 10µm. (d) Quantification of cells with pATM and 53BP1 foci in the experiment in (c). ns, non-significant.

not significant. Error bars indicate s.d. (e) Protein extracts from cells left untreated or treated with IR as in (c), blotted and probed with the indicated antibodies. Experiments were replicated at least twice.

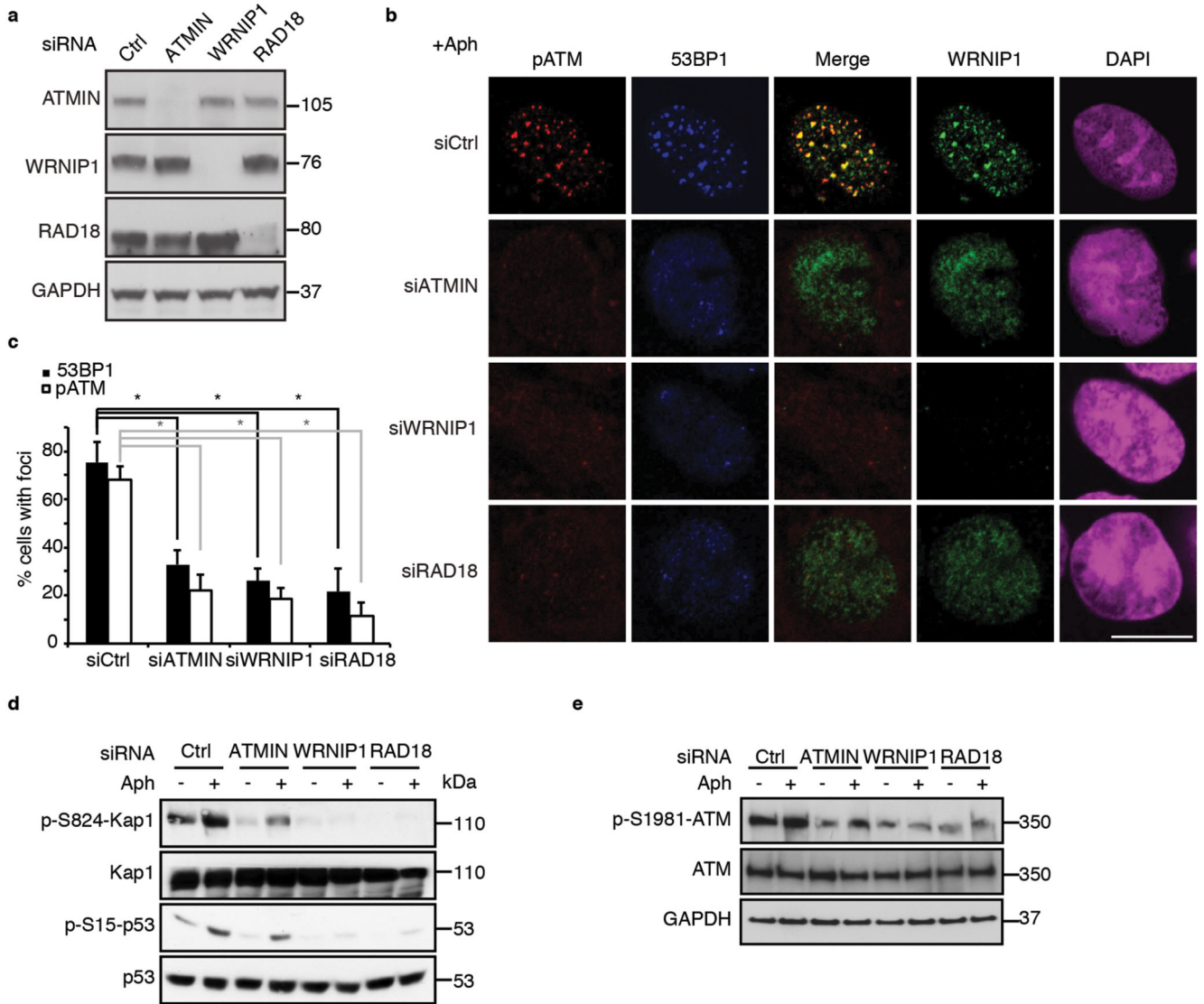


**Figure 4. WRNIP1, ATMIN, and RAD18 are required for ATM signalling in response to aphidicolin**  
 (a) Western blots showing knockdown of ATMIN, WRNIP1 and RAD18 by siRNA. (b) Disruption of 53BP1 and pATM recruitment following siRNA depletion of WRNIP1, ATMIN and RAD18 in HEK293 cells fixed and stained with the indicated antibodies after exposure to 0.2 $\mu$ M aphidicolin for 24 hours. siCtrl, siRNA control. Scale bar indicates 10 $\mu$ m. (c) Quantification of the percentage of cells in (b) with 53BP1 or pATM foci. \*, p<0.05 (t-test). At least 100 cells were counted per condition. Error bars represent s.d. (d) Western blots showing compromised aphidicolin-induced ATM signalling in the absence of ATMIN, WRNIP1 or RAD18, using extracts from HEK293T cells transfected with siRNAs as above and left untreated or treated with 2 $\mu$ M aphidicolin for two hours. (e) Western blots assessing ATM auto-phosphorylation (pATM) and total ATM in cells treated as in (d). Experiments were replicated three times.

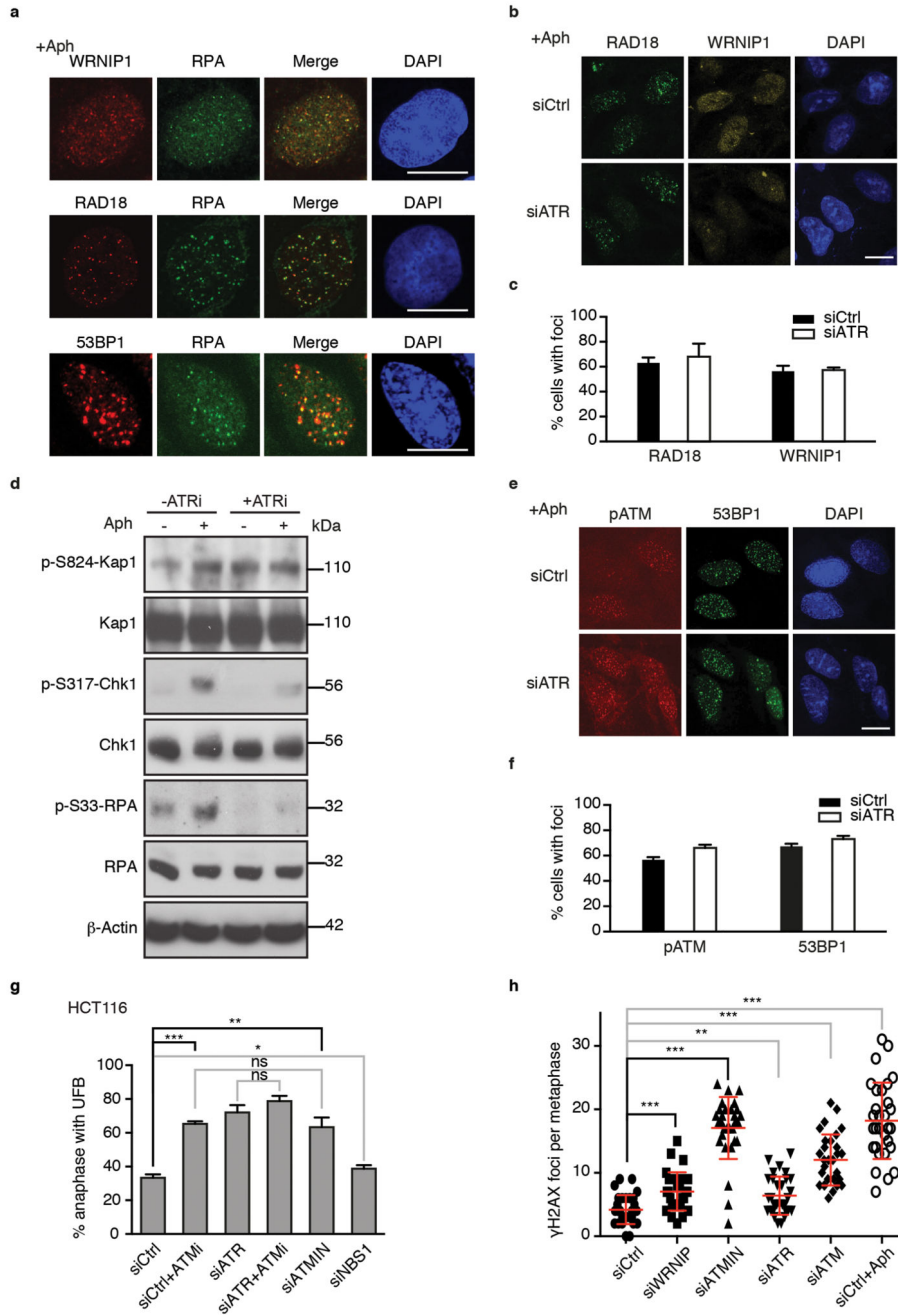


**Figure 5. Aphidicolin-induced ATM signalling is not impaired in ATR-deficient cells, but depletion of ATMIN increases unresolved damage at mitosis**

(a) HEK293A cells stained with antibodies against WRNIP1, RPA, 53BP1 and Rad18 after treatment with 0.2  $\mu$ M aphidicolin for 24 hours. (b) HCT116 cells transfected with control siRNA (siCtrl) or siRNA against ATR, treated with aphidicolin as above and stained with WRNIP1 or RAD18 antibodies. (c) Quantification of RAD18 and WRNIP1 foci in the experiment in (b). Error bars indicate s.d. (d) Western blots showing phosphorylation of Kap1 in untreated HEK293 cells or cells treated with ATR inhibitor (ATRI) and/or 2  $\mu$ M aphidicolin for 2 hours. Chk1 and RPA phosphorylation are shown as positive controls for

ATR inhibition. Experiment was replicated twice. (e) HCT116 cells treated with siRNA and 0.2  $\mu$ M aphidicolin for 24 hours as in (b) and stained with pATM and 53BP1. (f) Quantification of pATM and 53BP1 foci in the experiment in (e). Error bars indicate s.d. (g) Quantification of the percentage of anaphases with at least one ultrafine bridge (UFB) in HCT116 cells treated with control siRNA (siCtrl) or siRNA against ATMIN, ATR, or NBS1, with 10  $\mu$ M ATM inhibitor KU55933 where indicated (ATMi). (h) Quantification of  $\gamma$ H2AX foci in metaphase cells treated with the indicated siRNAs. ns=not significant; \*p=0.0349; \*\*p=0.0011 (g) or p=0.0024 (h); \*\*\*p=0.0001 (unpaired t-test). Scale bars represent 10 $\mu$ m. Error bars represent s.d.